Molecular Crystals and Liquid Crystals
Publication details, including instructions for authors and subscription information:
http://www.tandfonline.com/loi/gmcl20

The Effect of Filler Morphology and Distribution on Electrical and Shielding Properties of Graphite-Epoxy Composites

L. L. Vovchenko [a], L. Yu. Matzui [a], V. V. Oliynyk [b] & V. L. Launetz [b]
[a] Faculties of Physics, Taras Shevchenko National University of Kyiv, Kyiv, Ukraine
[b] Radiophysics, Taras Shevchenko National University of Kyiv, Kyiv, Ukraine

Version of record first published: 03 Mar 2011

To cite this article: L. L. Vovchenko, L. Yu. Matzui, V. V. Oliynyk & V. L. Launetz (2011): The Effect of Filler Morphology and Distribution on Electrical and Shielding Properties of Graphite-Epoxy Composites, Molecular Crystals and Liquid Crystals, 535:1, 179-188

To link to this article: http://dx.doi.org/10.1080/15421406.2011.538335

Mol. Cryst. Liq. Cryst., Vol. 535: pp. 179–188, 2011

ISSN: 1542-1406 print/1563-5287 online
DOI: 10.1080/15421406.2011.538335

Taylor & Francis
Taylor & Francis Group

The Effect of Filler Morphology and Distribution on Electrical and Shielding Properties of Graphite-Epoxy Composites

L. L. VOVCHENKO,[1] L. YU. MATZUI,[1]
V. V. OLIYNYK,[2] AND V. L. LAUNETZ[2]

[1]Faculties of Physics, Taras Shevchenko National University of Kyiv, Kyiv, Ukraine
[2]Radiophysics, Taras Shevchenko National University of Kyiv, Kyiv, Ukraine

A comparative study of epoxy resin filled with thermoexfoliated graphite (TEG) of various dispersities has been carried out to investigate the effect of filler particle's morphology on electromagnetic interference (EMI) shielding properties of composites within the 25.86–37.5 GHz frequency range of electromagnetic radiation. The shielding properties of a multilayered structure (LS) of TEG-epoxy presenting the set of alternating layers of TEG and epoxy have been investigated as well. The total content of TEG in this multilayered structure was 0.8 and 3 wt.%. It is found that the composites containing TEG exhibit enhancements in the electrical conductivity and the electromagnetic shielding efficiency as compared with those of composites with sonicated TEG.

Keywords Dielectric permittivity; electromagnetic shielding; graphite nanoplatelets; porosity; reflection and absorption loss

Introduction

The problem of the protection of people against the increase of the total electromagnetic field intensity in the environment, especially that of the population in the industrial regions, is currently an urgent problem. Properties required for "universal" electromagnetic interference (EMI) shielding materials are high absorbing characteristics, high resistance to the environmental erosion, high mechanical strength, and good adhesion to a metallic substrate. The materials should be also thin and light. Recently, it became clear that nanostructured conducting components embedded in a dielectric medium can be a new class of broad-band electromagnetic absorption materials [1–5]. The application of different polymers as a dielectric matrix allows one to create shielding materials possessing a qualitatively different set of structural and mechanical characteristics, temperature range of operation,

Address correspondence to L. L. Vovchenko, Faculties of Physics, Taras Shevchenko National University of Kyiv, 64 Volodymyrska, Kyiv 01033, Ukraine. E-mail: vovch@univ.kiev.ua

etc. Polymers can be easily processed and fabricated into intricately shaped components without damaging a structure of fillers during the processing using conventional methods, and, hence, the fabrication cost can be certainly reduced. Understanding the EMI shielding mechanisms of polymer composite materials (CMs) is essential for the best utilization of the EMR shielding capabilities of CMs and for designing the composites at the lowest possible filler loading and cost. Conductive polymer composites containing conductive nanostructured fillers with a high aspect ratio are characterized by a sufficiently low percolation threshold in the electric conductivity. This allows one to save the technological advantages of polymer matrices. Nanocarbon-based polymer composites stimulate a great interest and have been extensively investigated [6–8]. The analysis of the results of these researches shows that the performance of these composites depends on many factors such as the type of nanocarbon fillers (SWNTs or MWCNTs, graphite nanosheets, etc.), their morphology and structure (e.g., diameter, length, and chirality of CNT), the processing method, the choice of a matrix [5,9,10], the nanocarbon dispersion within a matrix [11,12], the interfacial interaction between nanocarbon and a matrix, etc. One more important problem is to find a correlation between the structure, morphology, and phase composition of constituents and the properties of polymer composites in the medium, high, and superhigh frequency ranges, since this will allow one to select an optimal composition of composites and to synthesise materials and structures possessing a wide range of electric parameters. The aim of this study is to establish the influence of filler's morphology and its spatial distribution (including the fabrication of polymer-fillers with a multilayered structure) on the shielding properties of epoxy-graphite composites.

Experimental

We investigate the composite materials based on epoxy resin and various types of graphite filler: disperse graphite, thermoexfoliated graphite (TEG), TEG2 (TEG subjected to repeated oxidation and thermoexfoliation), dispersed TEG2d, and nanoTEG (TEG2 and TEG subjected to ultrasonic dispersing during 3 and 20 h, respectively). The epoxy-based composites have been prepared by the method described in [13].

We also fabricate the multilayered structures (LS) of TEG-epoxy presenting the set of alternating layers of TEG and epoxy, the number of TEG and epoxy layers being 7 and 8, respectively. The total content of TEG in these multilayered structures was 3 (N1) and 0.8 wt.% (N2). Figure 1 shows the light microscopy image of a multilayered structure N1 TEG-epoxy and its schematic presentation.

The estimated thickness of epoxy layers was approximately 400 μm, while the thickness of graphite layers was ~40 and ~20 μm for multilayered structures N1 and N2, respectively. Such a thickness of graphite layers testifies to a low density of graphite layers, especially in the case of multilayered structure N2. It is possible that such graphite layers are not continuous (compact).

The specimens of TEG-epoxy composites and multilayered structures in the form of $7.2 \times 3.4 \times (1–3.4)\,mm^3$ plates were prepared to analyze the interaction of electromagnetic radiation with the studied materials. Such sample's shape allows one to cover a section of a rectangular copper waveguide. A standard P2-65 device (Lithuania, the equivalent of a microwave network analyzer) was used to measure the transmission coefficient within the 25.86–37.5 GHz frequency range. Voltage

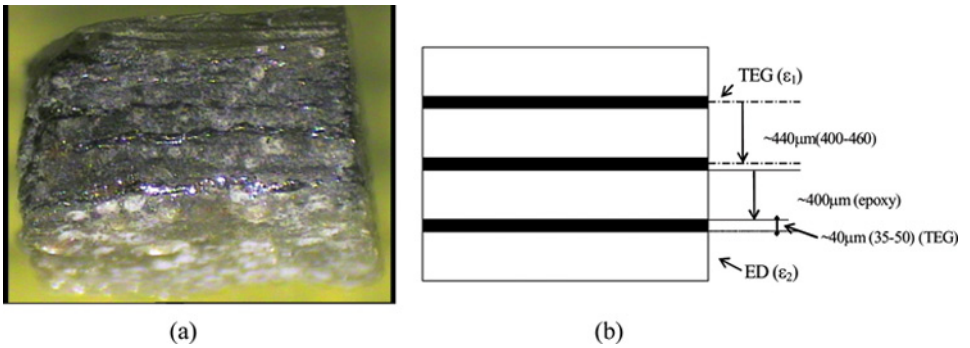

Figure 1. The light microscopy image (a) and schematic presentation (b) of a multilayered structure of TEG-epoxy.

measurements of the standing wave ratio (SWR) [12] were used to determine the reflection properties and the complex dielectric permittivity of the studied specimens. This method allows us to avoid errors arising due to deviations from the quadratic law of characteristics of SHF-detectors used in the measuring SHF installations. The essence of the method of determination of the permittivity is described in [14].

Results and Discussion

The electrical conductivity of the investigated epoxy composites obeys the percolation law, but the characteristics of the percolation transition (percolation threshold and transition width) depend on the morphology of graphite fillers, such as the particle's shape and size (aspect ratio). The data on fillers' morphology are listed in Table 1.

The difference in morphology of used fillers leads to different spatial distribution of graphite fillers in epoxy matrix that effect on percolation threshold in electrical

Table 1. Electrical conductivity, EMR reflection, absorption and transmission coefficients in epoxy based composites with 10 wt.% of graphite filler

CM with 10 wt.% of graphite filler	Gr Platelets, 50 μm (diameter) 5–30μm (thickness)	TEG Worms, 3–5 mm (length) 50–100 μm (diameter)	TEG2 Particles, 0.3–0.5 mm (thickness) 50–100 μm (diameter)	TEG2d	nanoTEG Platelets, 40–130 nm (thickness); 0.1–10 μm (diameter)
σ_{dc}, S/m	$5 \cdot 10^{-8}$	300	130	20	$9 \cdot 10^{-2}$
		f = 27 GHz, h = 0.7 mm			
R	0.60	0.68	0.67	0.67	0.63
A	0.196	0.320	0.329	0.302	0.297
T	0.204	$1.26 \cdot 10^{-4}$	$1.18 \cdot 10^{-3}$	$2.75 \cdot 10^{-2}$	$8.32 \cdot 10^{-2}$
SE_A, (-dB)	2.9	34.1	24.5	10.8	6.6

conductivity. As was shown in [13], the lower percolation threshold was observed for TEG-ED composites. When the dispersion of particles increases in the row TEG → TEG2 → TEG2d → nanoTEG, the percolation transition shifts to a higher content of the graphite filler: $C_{cr} = 0.9 \rightarrow 2.9 \rightarrow 3.2 \rightarrow 6.4 \rightarrow 25$ wt.%. For example, in CMs with disperse graphite, the percolation transition is sufficiently wide (~17–32 wt.%), and C_{cr} is equal approximately to 25 wt.%. Hence, at equal weight contents of graphite components with various morphologies, the electrical conductivity of CMs will be different. Table 1 presents data on the electrical conductivity for epoxy composites with 10 wt.% of the graphite component.

As seen, the electrical conductivity of CM with TEG is by 6 orders higher than that in CM with dispersed graphite. This difference testifies to the essential role of the filler particles' morphology, their distribution in the epoxy matrix, and the ability to structuring (the formation of chains and the skeleton structure) for the electrical conductivity of CMs.

Now let us consider the investigated EMI shielding properties for graphite-epoxy composites.

Using the electromagnetic radiation power balance equation and measuring experimentally the powers of reflected R and transmitted T waves, we can determine the power of absorbed (A) waves in the CM bulk [12]:

$$I = R + A + T, \quad R = |E_I'/E_I|^2, \quad T = |E_T/E_I|^2 \tag{1}$$

where I is the power of incident waves, and it may be set as $I = 1$; E_I, E_I', E_T are the values of electric field of incident, reflected and transmitted waves, respectively.

The reflection loss RL (in dB), experimentally measured standing wave ratio (SWR), and the power of reflected waves R are connected by the formulas

$$SWR = \frac{1 + 10^{-\frac{RL}{20}}}{1 - 10^{-\frac{RL}{20}}}, \quad RL = 10 \log \frac{R}{I} = 10 \log R. \tag{2}$$

The total EMI shielding efficiency SE_T (in dB) is defined as

$$SE_T = SE_R + SE_A = 10 \log \frac{T}{I}; \tag{3}$$

where SE_R and SE_A are the shielding efficiencies due to reflection and absorption of electromagnetic radiation in material:

$$SE_R = 10 \log \frac{I - R}{I}; \quad SE_A = 10 \log \frac{T}{I - R} \tag{4}$$

Figure 2 shows the EMI transmission coefficient (SE_T) for these CMs. As was shown in our previous paper [13,14], the attenuation of EMI is proportional to the electrical conductivity of CM. Comparing the data of Table 1 and Figure 2, it can be concluded that the values of EMI transmission coefficient for the epoxy composites with 10 wt.% of various graphite fillers correlate with their electrical conductivity.

The obtained results confirm the conclusion that the composite conductivity (mainly determined by the connectivity of conducting filler particles) is an important

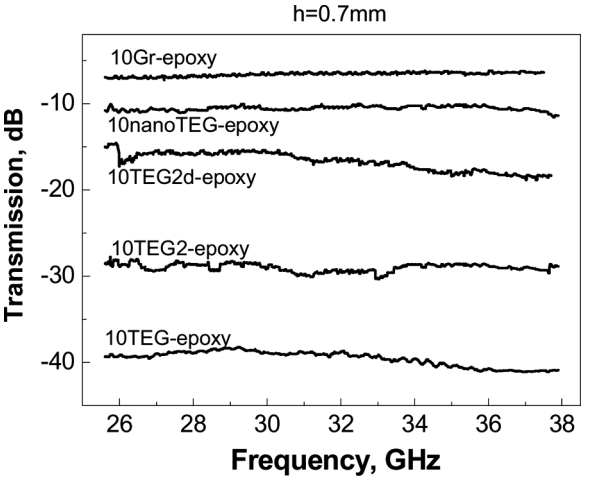

Figure 2. The coefficient of EMR transmission for epoxy-based CMs with graphite fillers of different morphologies versus the EMR frequency.

factor in addition to the filler intrinsic conductivity and the concentration which provide a high EMI attenuation due to the processes of reflection and absorption of electromagnetic waves.

For the solid conducting medium, the primary mechanism of EMI shielding is the reflection. In heterogeneous structures such as filled polymers, the role of EMI absorption in CM increases sufficiently, and the reflection R decreases as compared with that of a solid conducting shield. As we have shown in our previous work [15], the EMI reflection coefficient R in the frequency range 25–37 GHz for pure dense TEG is high and equal to 0.86, whereas, for the epoxy CMs with 2–10 wt.% TEG, R achieves only 0.6–0.67. Generally, it may be concluded that the EMI reflection coefficient R in the materials with TEG depends on the boundary layer state (about 40 μm) of the shield. It is obvious that the denser boundary layer leads to a higher level of the orientation of graphite particles in the shield's plane (i.e., the higher electrical conductivity in the $\vec{E}$-direction of a wave). Subsequently, the EMI reflection coefficient R increases. That is why in polymer composites with a low content of TEG, the EMI reflection coefficient is lower as compared with that of pure compacted TEG (see Table 1). As seen from Table 1, the absorption losses correlate with the values of electrical conductivity of CMs with 10 wt.% of graphite fillers: SE_A is maximal for composite with 10 wt.% of TEG and is minimal for CM with 10 wt.% of dispersed graphite.

Now, we will show that the shielding efficiency against EMI of the TEG-epoxy composites depends not only on the TEG content in a TEG-epoxy composite material but on the fabrication method of the composites. Figure 3a,b present the reflection loss RL and the EMI shielding efficiency SE_T in multilayered structure TEG-ED (N1) for various dispositions of the multilayered shield relative to the direction of electromagnetic radiation propagation.

It is found that the highest values of shielding efficiency are observed for such a disposition of the multilayered shield when the electric field vector $\vec{E}$ lies in the plane of TEG layers. For another disposition of shields, when $\vec{E}$ is orthogonal to graphite layers, the EMI shielding efficiency is low, and the peculiarities on the frequency

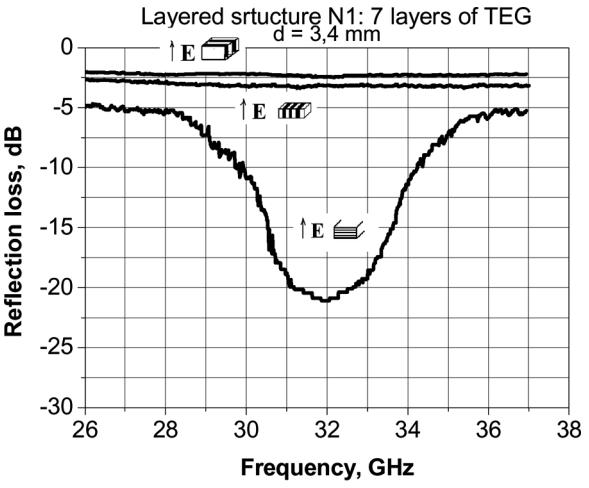

(a)

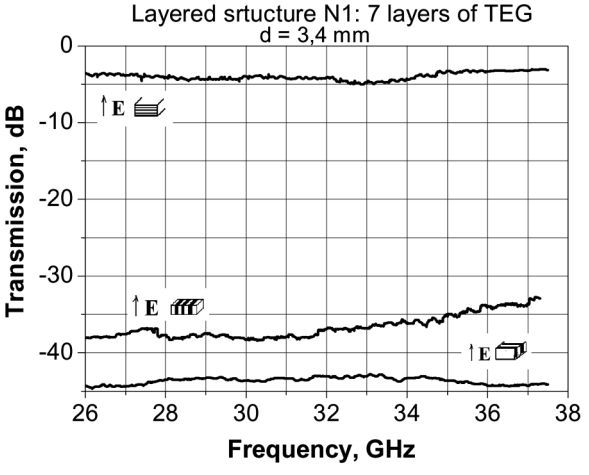

(b)

Figure 3. The coefficient of EMR reflection loss and the shielding efficiency SE_T for multilayered structure of TEG-epoxy as a function of the electromagnetic radiation frequency for various dispositions of the multilayered shield relative to the direction of electromagnetic radiation propagation.

dependence of reflection losses arise: the minimum of *RL* is observed at an electromagnetic radiation frequency of about 30 GHz.

Table 2 lists the contributions of reflection and absorption to the overall EMI SE for a bulk specimen of pure TEG with a thickness ~0.25 mm and for multilayered structures TEG-ED with the total thickness of 7 TEG layers ~0.28 mm. As seen from Table 2, the multilayered structures are characterized by a higher value of EMI shielding efficiency (−44 dB and −28 dB for LS N1 and LS N2, respectively) despite the lower values of reflection loss as compared with those of pure bulk TEG. It must be mentioned also that the density of TEG layers in LS is sufficiently

Table 2. The shielding characteristics of layered structures of TEG-epoxy and bulk pure TEG

Material type	Total thickness of TEG layers, μm	Porosity of individual graphite layer	SE_R, (-dB)	SE_A (-dB)	SE_T (-dB)
			f = 27 GHz, $\vec{E}$ lies in the plane of a graphite layer		
LS TEG-ED N1	~280	0.90	4.1	40.3	44.4
LS TEG-ED N2	~260	0.95	5.5	23.3	28.8
Bulk pure TEG, h = 0.25 mm	~250	0.10	8.6	12.0	20.7

lower than that of bulk TEG (see Table 2). In other words, the amount of the electroconducting graphite phase responsible for the reflection and absorption losses is lower in the case of LS. The high value of EMI shielding efficiency SE_T in LS can be explained by the reflection of electromagnetic radiation inside of LS from a few graphite layers (from additional surfaces), which leads to an increase of SE_A in comparison with that of a monolithic TEG plate, where only two reflecting planes exist.

The investigated multilayered structure can be modeled by a multilayered medium with dielectric permittivity ε and permeability μ varying as a function of z, where the electromagnetic properties are approximately constant in each region (Fig. 1). The incident wave in the waveguide, H_{10}, can be presented as a plane wave with the electric and magnetic fields

$$\begin{aligned} &\vec{E}_p = \vec{e}_y \cdot A \cdot e^{ik_z z}; \quad \vec{H}_p = \vec{e}_x \cdot \frac{1}{Z} A \cdot e^{ik_z z}; \\ &Z = 120\pi \Big/ \sqrt{\varepsilon\mu - \left(\frac{\lambda_0}{2a}\right)^2}; \quad k_z = \frac{2\pi}{\lambda} \cdot \sqrt{\varepsilon\mu - \left(\frac{\lambda_0}{2a}\right)^2}, \end{aligned} \tag{5}$$

where Z is the infinite waveguide impedance, k_z is the propagation constant, z is the direction of electromagnetic radiation transmission, and λ is the wavelength.

The fields reflected from the shielding structure are as follows:

$$\vec{E}_p^- = \vec{e}_y \cdot C \cdot e^{ik_z z} \quad \vec{H}_p^- = -\vec{e}_x \cdot \frac{1}{Z} C \cdot e^{ik_z z}. \tag{6}$$

Analogously, the fields in the n-th layer are

$$\begin{aligned} &\vec{E}_n = \vec{e}_y \cdot B_n \cdot e^{ik_{zn} z}; \ \vec{H}_n = \vec{e}_x \cdot \frac{1}{Z_n} B_n \cdot e^{ik_{zn} z}; \\ &\vec{E}_n^- = \vec{e}_y \cdot B_n \cdot e^{ik_{zn} z}; \ \vec{H}_n^- = -\vec{e}_x \cdot \frac{1}{Z_n} B_n \cdot e^{ik_{zn} z}, \end{aligned} \tag{7}$$

where $k_{zn} = \frac{2\pi}{\lambda} \cdot \sqrt{\varepsilon_n \mu_n - \left(\frac{\lambda_0}{2a}\right)^2}$ is the wave impedance of the waveguide with the shield with parameters ε and μ; A, B_n, C are the amplitudes of the fields, $2a$ is the

larger dimension of the waveguide, and

$$k_{z1} \cdot d_1 + k_{z2} \cdot d_2 + k_{z3} \cdot d_3 + \cdots + k_{z(n-1)} \cdot d_{(n-1)} \leq k_{zn} \cdot d_n \leq k_{zn+1} \cdot d_{n+1} + \cdots + k_{zN} \cdot d_N, \tag{8}$$

where d_n is the thickness of the n-th layer.

Taking the absorption processes in materials into account, the dielectric permittivity can be presented as $\varepsilon_n = \varepsilon'_n + i\varepsilon''_n$. For nonmagnetic materials ($\mu = 1$), the propagation constant is described by the relation $k_{zn} = k_{zn} + i\alpha_n$, where α_n is the absorption coefficient in the n-th layer. The boundary conditions for the electric and magnetic fields on the surface of each plate (layer) give the necessary number of equations for all unknown parameters. So, for N layers, we have the system of $2N$ linear equations and the same number of the unknown parameters. We have numerically calculated the EMI transmission coefficient $SE_T(dB)$ (the coefficient α is not considered) for LS TEG-epoxy in the case where the graphite layers are perpendicular to the EMR propagation direction (Fig. 4).

The results of our calculations have shown that, in the case of the bulk TEG shield (one plate) with thickness $n \cdot d$, the value of SE_T is lower than that in multilayered structures TEG-epoxy, where the total thickness of n graphite layers is the same, i.e., $n \cdot d$. It was found that the value of shielding efficiency and its dependence on the electromagnetic radiation frequency for LS are determined by the number and the thickness of TEG and epoxy layers. It was found also that a deviation from the identity of graphite (or epoxy) layers (various thicknesses of TEG (or epoxy) layers) may lead to changes in the value of $SE_T(dB)$ and its specific dependence on the EMR

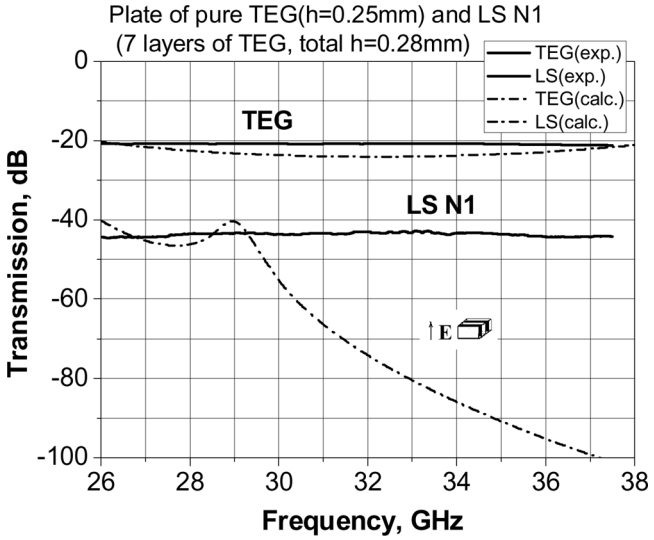

Figure 4. The coefficient of EMR transmission *versus* the frequency for bulk pure TEG ($h = 0.25$ mm) and multilayered structure N1 (the total thickness of 7 graphite layers is equal $\sim$0.28 mm, the thickness of an individual epoxy layer is 0.4 mm): solid line – experiment, dash-dotted line – calculated curves at $\varepsilon'_{Gr} = 753, \varepsilon'_{epoxy} = 4.16$; graphite layers are perpendicular to the direction of electromagnetic radiation propagation.

frequency. The imperfection of TEG layers and their inhomogeneity as for the thickness and the density leads to the smoothing of possible sharp minima and maxima on $SE_T(f)$ caused by the periodicity of multilayered structures. In addition, it is necessary to consider the energy loss (coefficient α) in the material to attain the better agreement between the experimental and calculated values of SE_T. A more detailed consideration of multilayered structures based on TEG and epoxy will be performed in our future work.

Conclusion

It is found that the composites containing TEG or TEG2 with skeleton structure exhibit enhancements in the electrical conductivity and the electromagnetic interference shielding efficiency as compared with those of composites with dispersed graphite (Gr) and sonicated TEG2d and nanoTEG. The composite conductivity (mainly determined by the connectivity of conducting filler particles) is an important factor in addition to the filler intrinsic conductivity and the concentration which provide the high EMI shielding characteristics. The comparative study of bulk composites and multilayered structures of TEG-epoxy has shown that the filler distribution in the epoxy matrix influences the electromagnetic shielding efficiency: it is maximal for a multilayered structure where the graphite layers are perpendicular to the direction of electromagnetic radiation propagation. The shielding properties of multilayered structures TEG-epoxy are enhanced as compared with those of monolithic CMs with the same mass content of TEG due to the multiple EMR reflection from additional surfaces in multilayered structures. The modeling of the investigated multilayered structure by a multilayered medium with dielectric permittivity ε and permeability μ varying as a function of z has shown that the value of shielding efficiency SE_T is proportional to the number and the thickness of TEG and epoxy layers. The deviation from the identity of graphite (or epoxy) layers may lead to changes in the value of SE_T and its specific dependence on the electromagnetic radiation frequency.

Acknowledgment

This work was supported by the STCU grant N4908.

References

[1] Che, R. C., Peng, L. M., Duan, X. F., Chen, Q., & Liang, X. L. (2004). *Adv. Mater.*, *16*(5), 401.
[2] Yang, Y. L., & Gupta, M. C. (2005). *Nanoletters*, *5*, 2131.
[3] Cao, M.-S., Song, W.-L., Hou, Z.-L., Wen, B., & Yuan, J. (2010). *Carbon*, *48*, 788.
[4] Liu, X. G., Ou, Z. Q., Geng, D. Y., Han, Z., Jiang, J. J., Liu, W., & Zhang, Z. D. (2010). *Carbon*, *48*, 891.
[5] Park, K.-Y., Lee, S.-E., Kim, C.-G., & Han, J.-H. (2006). *Compos. Sci. Techn.*, *66*, 576.
[6] Grunlan, J. C., Mehrabi, A. R., Bannon, M. V., & Bahr, J. L. (2004). *Adv. Mater.*, *16*(2), 150.
[7] Gojny, F. H., Nastalczyk, J., Roslaniec, Z., & Schulte, K. (2003). *Chem. Phys. Letters*, *370*, 820.

[8] Maksimenko, S. A., Rodionova, V. N., Slepyan, G. Ya., Karpovich, V. A., Shenderova, O., Walsh, J., Kuznetsov, V. L., Mazov, I. N., Moseenkov, S. I., Okotrub, A. V., & Lambin, Ph. (2007). *Diamond and Related Materials*, *16*, 1231.
[9] Wang, T., Chen, G., Wu, C., & Wu, D. (2007). *Progress in Organic Coatings*, *59*, 101.
[10] Yuen, S.-M., Ma, C.-C. M., Chuang, C.-Y., Yu, K.-C., Wu, S.-Y., Yang, C.-C., & Wei, M.-H. (2008). *Compos. Sci. Techn.*, *68*, 963.
[11] Panwar, V., Kang, B., Park, J.-O., Park, S., & Mehra, R. M. (2009). *Europ. Polymer Journ.*, *45*, 1777.
[12] Al-Saleh, M. H., & Sundararaj, U. (2009). *Carbon*, *47*, 1738.
[13] Vovchenko, L., Matzui, L., Oliynyk, V., & Launetz, V. (2010). *Physica Status Solidi C*, *7*, 1260.
[14] Vovchenko, L., Matzui, L., Oliynyk, V., Launetz, V., & Lazarenko, A. (2008). *Mol. Cryst. Liq. Cryst.*, *497*, 378.
[15] Vovchenko, L., Matzui, L., Oliynyk, V., Launetz, V., Prylutskyy, Yu., Hui, D., & Strzhemechny, Yu. (2008). *Int. Journ. Nanoscience*, *7*, 263.